(Scheringer, 1977). $1-\beta$ describes the relative contribution of the internal modes. In principle, $1-\beta$ is different for each component $ij$ and for each atom, but in order to obtain representative results we consider only the averages already described (Table 3). At 300 K the $1-\beta$ values of the C, N, O atoms are small (1·8%). For benzene, naphthalene and anthracene values of 1·7, 3·2 and 6·8% respectively were found for the C atoms at 292 K (Scheringer, 1972). At 98 and 60 K the $1-\beta$ values of the C, N, O atoms in urea increase due to the decrease of the external modes, but they remain small (<6%). For the H atoms we find large relative contributions of the internal modes to the vibration tensors at all temperatures (Table 3). The reason for this is that the H atoms chiefly take part in the out-of-plane modes with low frequencies. The large $1-\beta$ values found for the H atoms in benzene, naphthalene and anthracene (11·8, 22·4 and 39·1% respectively at $T=292$ K; Scheringer, 1972) seem to confirm our results for urea.

Scheringer (1977) estimated $1-\beta \simeq 25\%$ at 100 K for the first-row elements in molecules of medium size. This investigation shows that, for urea, this estimate is much too high. The discrepancy is partly due to the fact that the molecules considered earlier were larger than urea. The four relevant atoms, C, O, N(1), N(2), in urea form a very small unit in space, to the motions of which only the higher internal frequencies can contribute.

Since, for urea, the internal modes contribute little to the Debye–Waller factors of the C, N, O atoms, we conclude that the model of rigid-body motions will give a useful description for the motions of these atoms down to 60 K. The relative errors made with the rigid-body model will then be <10% of the vibration tensors of the C, N, O atoms. The rigid-body approximation obviously cannot be applied to the H atoms. Similarly, for larger molecules like anthracene, with some low-frequency internal modes, the rigid-body approximation will no longer be appropriate for any atom at 100 K.

M. Ishii thanks the Alexander-von-Humboldt-Stiftung, Bonn, for the award of a research scholarship.

### References


DUNCAN, J. L. (1971). *Spectrochim. Acta Part A*, **27**, 1197–1205.

HADŽI, D., KIDRIČ, J., KNEŽEVIC, Z. V. & BARLIČ, B. (1976). *Spectrochim. Acta Part A*, **32**, 693–704.

HEGER, G., MULLEN, D. & TREUTMANN, W. (1979). To be published.

PRYOR, A. W. & SANGER, P. L. (1970). *Acta Cryst.* A**26**, 543–558.

SAITO, Y., MACHIDA, K. & UNO, T. (1971). *Spectrochim. Acta Part A*, **27**, 991–1002.

SCHERINGER, C. (1972). *Acta Cryst.* A**28**, 516–522.

SCHERINGER, C. (1973). *Acta Cryst.* A**29**, 82–86.

SCHERINGER, C. (1977). *Acta Cryst.* A**33**, 426–429, 430–433.

SCHERINGER, C. & FADINI, A. (1979). *Acta Cryst.* A**35**, 610–613.

SHIMANOUCHI, T. (1968). Univ. of Tokyo.

SHTEINBERG, B. YA., MUSHKIN, YU. I. & FINKELSHTEIN, A. I. (1972). *Opt. Spectrosc.* **33**, 589–592.

YAMAGUCHI, A., MIYAZAWA, T., SHIMANOUCHI, T. & MIZUSHIMA, S. (1957). *Spectrochim. Acta*, **10**, 170–178.


*Acta Cryst.* (1979). A**35**, 616–621

# A Limited-Range Step-Scan Method for Collecting X-ray Diffraction Data

BY JONATHAN C. HANSON,* KEITH D. WATENPAUGH, LARRY SIEKER AND LYLE H. JENSEN

*Department of Biological Structure, University of Washington, Seattle, Washington* 98195, *USA*

(*Received* 1 *October* 1976; *accepted* 19 *February* 1979)


### Abstract

A limited-range, step-scan method for rapid diffractometer data collection is described. The data are reduced in a two-pass procedure. First, the step data from the more intense peaks are fitted by a Gaussian function $y_i = C_1 \exp[-(\bar{x}-x_i)^2/C_2^2]$, where $C_1$ is the peak maximum, $C_2$ is proportional to the peak width and $C_1C_2$ is proportional to the integrated intensity. Because the peak widths may vary appreciably over the range of data observed and cannot be determined very precisely for weak reflections, an empirical function is determined from the more intense reflections in the first pass and the calculated peak widths are used for all reflections in the second pass. Comparison of data


* Present address: Biology Department, Brookhaven National Laboratory, Upton, New York 11973, USA.

0567-7394/79/040616-06$01.00 

obtained by this method and the usual full-scan technique shows that comparable precision can be obtained even when the limited scan range data are collected at twice the rate of the full-scan technique. The method has been used to collect data for five proteins and typical results are cited.

## Introduction

The limited-range, step-scan method of collecting X-ray data described here was developed to meet the special characteristics of protein crystals. Such crystals can suffer extensive radiation damage in the X-ray beam, and it is important to minimize the effects of deterioration by maximizing the data acquisition rate. Furthermore, the integrated intensities for protein crystals are relatively weak and decrease rapidly with increasing diffraction angle because of the large unit cells and the high 'thermal' parameters of the atoms. It is important, therefore, to choose a counting scheme that will achieve as high a signal-to-noise ratio as possible.

The stationary-crystal, stationary-counter method has been used to meet the above requirements. However, with the dimensions common for present diffractometers, integration may be incomplete for large crystals even for the highest convergence of the beam that can normally be attained. Moreover, protein crystals are susceptible to small changes in alignment because of the way they must be mounted, and along with inaccuracies in cell parameters, misalignment can lead to erroneous intensity measurements.

Wyckoff, Doscher, Tsernoglou, Inagami, Johnson, Hardman, Allwell, Kelly & Richards (1967) have described a limited-range, step-scan method that allows for setting and alignment errors by effectively broadening the peak plateau by dropping some steps and averaging over the remaining ones. The advantages are achieved at the expense of discarding considerable data, thus impairing the efficiency of the method and wasting crystal exposure time.

Diamond (1969) has devised a profile-fit, step-scan method leading to improved precision compared with other scan methods of collecting data, and he suggests that the method would be applicable to protein crystals. In this method, information about the peak profile is derived from the relatively intense reflections and used to determine the integrated intensities of the weak reflections. Lehmann & Larsen (1974) and Blessing, Coppens & Becker (1974) have developed profile analysis as applied to step-scan data, and Tickle (1975) has proposed a simplified method of treating step-scan data collected by computer-controlled diffractometers.

The method described here requires only a limited number of steps in the scan because a functional form of the peak is assumed. It is not as general, therefore, as the method proposed by Diamond (1969) which requires stepping completely across the peak, but it is rapid and achieves a high signal-to-noise ratio. Furthermore, it is suitable for crystals with large unit cells where adjacent reflections may seriously overlap unless precautions are taken to avoid the problem. Preliminary descriptions of the method have been given by Watenpaugh, Sieker, Jensen, LeGall & Dubourdieu (1972) and by Hanson, Watenpaugh, Sieker & Jensen (1973).

## The method in brief

In order to minimize the time for collecting data, counts are made only at a limited number of steps in the region near the peak maximum of each reflection. In order to further reduce the time of collecting data and to circumvent the effects of peak overlap for crystals with large unit cells, backgrounds may be assumed to be a function of $2\theta$ only and measured by scanning between selected reciprocal lattice rows.

The data are reduced in a two-pass procedure. In the first pass, the step-scan data for the more intense reflections are fitted by a Gaussian equation of the form $y_i = C_1 \exp[-(\bar{x} - x_i)^2/C_2^2]$, where $y_i = I_i - bk$ ($I_i$ is the count at $x_i$, $bk$ is the background count), $\bar{x}$ is the peak position in $2\theta$, $x_i$ is the $2\theta$ position of step $i$, $C_1$ is the peak height, and $C_2$ is proportional to the peak width.

For weak reflections, the precision of the width parameter $C_2$ is relatively low when the scan range is limited. Moreover, this parameter may vary over reciprocal space because of anisotropic mosaic structure and non-uniform crystal dimensions. In order to obtain a better estimate of $C_2$ for the weak reflections, we assume that it can be described by a seven parameter function for all reflections, the parameters being determined by fitting the $C_2$ of the more intense reflections in the first pass. Using this function, we calculate the width parameters for all reflections which are then used in the second pass through the data.

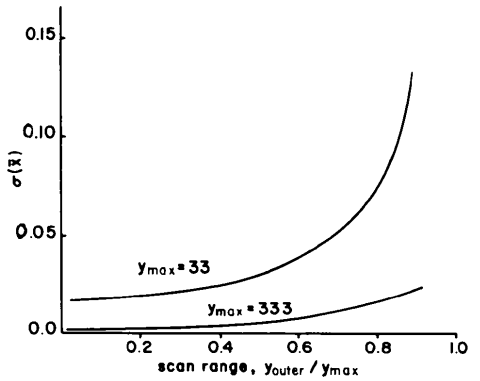


Fig. 1. Standard deviation of the peak center, $\bar{x}$, plotted as a function of different scan ranges. The scan range is given in terms of the ratio of $y_{outer}/y_{max}$. The curves represent the results obtained from two simulated reflections with five steps, backgrounds of 50 counts and maxima of 33 and 333 counts.

### The method in detail

In the first pass through the data, only reflections with all $y_i$ greater than some positive threshold value are used. This enables us to determine the parameters by least-squares calculations from the equations

$$z_i = \ln y_i = B_1 + B_2 x_i + B_3 x_i^2.*$$

Weights are taken as $1/\sigma(z_i)^2$ where $\sigma(z_i) = \sigma(y_i)/y_i = (I_i + bk)^{1/2}/y_i$. The $B_i$ and $\sigma(B_i)$ are used to calculate the profile parameters and their standard deviations according to the following equations:

$$C_1 = \exp[B_1 + (\bar{x}/C_2)^2],$$

$$\sigma(C_1) = C_1[\sigma^2(B_1) + (2\bar{x}/C_2^2)^2\sigma^2(\bar{x}) + (2\bar{x}^2/C_2^3)^2\sigma^2(C_2)]^{1/2},$$

$$\bar{x} = -B_2/2B_3,$$

$$\sigma(\bar{x}) = [(2B_3)^{-2}\sigma^2(B_2) + (B_2/2B_3^2)^2\sigma^2(B_3)]^{1/2},$$

$$C_2 = (-B_3)^{-1/2}, \quad \sigma(C_2) = 0{\cdot}5(-B_3)^{-3/2}\sigma(B_3).$$

The precision of the peak parameters depends on both the intensity of the reflection and the scan range. In order to illustrate the dependence of the precision of $\bar{x}$ on these factors, we describe the scan range in terms of the count of the outermost steps ($y_{outer}$) divided by the peak maxima ($y_{max}$). In Fig. 1, $\sigma(\bar{x})$ is plotted as a function of $y_{outer}/y_{max}$ for two reflections, one weak and one intermediate. It is evident from the plot that $\bar{x}$ can be determined within 0·03° even for very weak reflections if the scan extends to the point where the counting rate is half its value at the maximum.

To illustrate the dependence of the precision of the width parameter on scan range, we again describe the range in terms of $y_{outer}/y_{max}$, and Fig. 2 is a plot of $\sigma(C_2)/C_2$ *vs* this ratio for two reflections with maximum counts of 333 and 3333 and backgrounds of 50 counts. It can be seen that for the more intense reflection, $C_2$ can be determined to 5% relative precision by scanning to the point where the count is 0·8 of the peak maximum, but for the less intense reflection it is necessary to scan to the point where the intensity is 0·35 of the maximum to achieve the same precision.

From the above example, it is clear that a given peak width precision can be achieved by a much smaller scan range for the intense reflections than for the weak ones. By assuming a functional form for the width parameter and fitting it to the widths of the intense reflections determined in the first pass, we find that it is possible to limit the scan range and still maintain satisfactory precision in determining $C_2$. We express the width parameter by the function $C_2' = \sum\sum a_i a_j A_{ij} + k\tan\theta$, where the $a_i$ are the direction cosines of the diffraction vector relative to a Cartesian coordinate system fixed to the crystal, and $A_{ij}$ are elements of a symmetric tensor. This gives rise to a centrosymmetric ellipsoidal function for $C_2'$. The $k\tan\theta$ term is added to account for the contribution of the spectral dispersion to the peak width. The parameters $A_{ij}$ and $k$ are determined by a least-squares fit of the $C_2$ values determined in the first pass.

The width parameters for all reflections are calculated from the expression for $C_2'$ and used in the second pass through the data. For the more intense reflections, $C_1$ is determined by a least-squares fit to the $y_i$ with $\bar{x}$ fixed at the values determined in the first pass.* The expressions for $C_1$ and $\sigma(C_1)$ are the following:

$$C_1 = \sum[y_i \partial y_i/\partial C_1/\sigma^2(y_i)]/\sum[(\partial y_i/\partial C_1)^2/\sigma^2(y_i)],$$

$$\sigma(C_1) = [\sum(\partial y_i/\partial C_1)^2/\sigma(y_i)^2]^{-1/2},$$

and the integrated intensity on a relative scale from pass two is $C_1 C_2'$. All reflections are reduced in the second pass even though it would not be necessary for the more intense ones. For a reflection reduced in both passes, a weighted average of the two values is used.

### Tests of the limited-range, step-scan method

A preliminary version of the method described here in which $C_2$ was assumed isotropic was first used in collecting data for flavodoxin from *Desulfovibrio vulgaris* to 2·5 Å resolution (Watenpaugh *et al.*, 1972).

* An alternative method is to expand $y_i$ to first order in a Taylor series. This gives a better fit and is defined for $y_i \leq 0$.

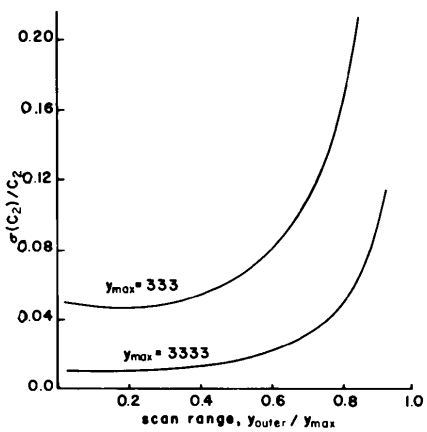


Fig. 2. For simulated reflections with five steps, background counts of 50 counts and peak maxima of 333 and 3333 counts, $\sigma(C_2)/C_2$ is plotted as a function of different scan ranges.

* For the less intense reflections, $\bar{x}$ was not determined by least-squares calculations. For these reflections the point with the greatest number of counts was considered to be equal to $\bar{x}$. This is a rough approximation, but will only have a small effect because the reflections are so weak. The best approximation would be obtained by determining an orientation matrix from $\bar{x}$ of the intense reflections in pass 1 and using it to evaluate $\bar{x}$ for the weak reflections in pass 2.

Table 1. *Peak width parameters and other information for several crystals*

Standard deviations are in units of the least significant figure.

| | Cytochrome cc'3 | Dipeptide* | *Glycera* Hemoglobin† | Azurin |
|---|---|---|---|---|
| $A_{11}$ | 0·1378 (3) | 0·2079 (11) | 0·321 (41) | 0·2410 (6) |
| $A_{12}$ | −0·0033 (3) | −0·0347 (12) | −0·048 (16) | 0·0001 (9) |
| $A_{13}$ | −0·0075 (3) | 0·0044 (9) | −0·048 (15) | −0·0472 (11) |
| $A_{22}$ | 0·1413 (3) | 0·1790 (30) | 0·220 (4) | 0·2246 (19) |
| $A_{23}$ | 0·0086 (3) | 0·0427 (20) | −0·010 (6) | −0·0101 (14) |
| $A_{33}$ | 0·1444 (4) | 0·1684 (21) | 0·2396 (2) | 0·3637 (30) |
| $k$ | −0·0020 (10) | 0·093 (12) | 0·0 | 0·0445 (18) |
| $S$‡ | 1·61 | 2·98 | 1·004 | 1·18 |
| Eigenvalues | 0·155 | 0·239 | 0·355 | 0·380 |
| | 0·136 | 0·195 | 0·241 | 0·228 |
| $A$ | 0·132 | 0·122 | 0·181 | 0·221 |
| $A_{iso}$ | 0·1356 (1) | 0·1798 (4) | – | – |
| $S_{iso}$ | 1·70 | 4·72 | – | – |
| No. of reflections | 3492 | 117 | 230 | 8310 |
| $d_{range}$ | ∞–4·0 Å | ∞–2·0 Å | 2·01–1·99 Å | ∞–2·7 Å |
| Radiation | Cu $K\alpha$ | Mo $K\alpha$ | Cu $K\alpha$ | Cu $K\alpha$ |
| Crystal dimensions | 0·3 × 0·3 × 0·3 mm | 0·1 × 0·06 × 0·5 mm | – | 0·4 × 0·56 × 0·6 mm |
| Tube take-off angle | 3·5° | 3·5° | – | 5·0° |

* D,L-Alanyl-D,L-methionine (Stenkamp & Jensen, 1974).
† Data collected with graphite monochromator.
‡ Standard deviation of an observation of unit weight.

In collecting the data from 2·5 to 2 Å, we used a modified version of the method since the $C_2$ parameter was found to be a function of $\chi$, which was allowed for in processing this part of the data (Watenpaugh, Sieker & Jensen, 1973).

Flavodoxin from *D. vulgaris* has a molecular weight of ~16 000 and crystallizes as well-formed octahedra, space group $P4_32_12$, unit cell parameters $a = b = 51{\cdot}6$, $c = 139{\cdot}6$ Å. The relatively large unit cell (~372 000 Å$^3$), together with the fact that ~60% of the cell volume is solvent would normally result in relatively weak intensities. Nevertheless, for the data in the range 2·5–2 Å we found only 5·4% of the reflections with $I < 2\sigma(I)$.

As a measure of the reproducibility of the flavodoxin data, the relative deviation from the mean intensity,

$$D_I = \sum_h \sum_i |\bar{I}_h - I_{ni}| / \sum_h n\bar{I}_h,$$

was 0·058 for the 6669 Friedel pairs in the range $2{\cdot}6 > d > 2$ Å for the native protein (negligible anomalous scattering). An additional indication of the reliability of the data is the fact that the structure was solved at 2·5 Å with a single-site $Sm^{3+}$ derivative by use of anomalous scattering data to resolve the phase ambiguity.

This method has also been used to collect native data for cytochrome cc'3 from *Desulfovibrio gigas* (Bruschi, LeGall, Hatchikian & Dubourdieu, 1969) (Table 1). The protein has molecular weight ~26 000 and crystallizes in space group $P3_1$ or $P3_2$ with unit cell parameters $a = b = 57{\cdot}4$, $c = 97{\cdot}3$ Å (Sieker & Jensen, 1971). Fast data collection is required because the intensities of the monitor reflections decrease at 0·5%/h. As a measure of the quality of the data, discrepancy indices were calculated between symmetry-related reflections which were in the zones located at the edge of the unique set of data. For 133 pairs of such reflections from the set of 3492 in the ∞ to 4·0 Å range, $D_I = 0{\cdot}053$.

### *Comparison with the full-scan method*

In order to compare the limited-range, step-scan method against the full-scan method, data have been collected by both techniques for cytochrome cc'3, for a dipeptide (Stenkamp & Jensen, 1974), and for carboxyhemoglobin from *Glycera dibranchiata* (Table 1).

For the cytochrome data, two sets of 400 reflections with $2\theta$ between 8 and 12° were collected, the step-scan being collected first followed immediately by the full-scan set. The latter was collected at a scan rate of 2°/min with a variable $2\theta$ scan range given by the expression $0{\cdot}82 + 0{\cdot}286 \tan\theta$ and 4 s background counts measured at the beginning and end of the scan range. The correction for crystal deterioration was by the expression $1{\cdot}0 + 3{\cdot}2 \times 10^{-5} \times$ reflection number, based on three reflections measured at the beginning and end of data collection. An empirical absorption correction was applied to both sets of data and had a range of 1·05 to 1·30. The limited-range, step-scan data were collected in five steps of 0·06° in $2\theta$ for 4 s/step. The empirical anisotropic width parameter

was determined from a slightly larger set of data on the same crystal. The $D_I$ index obtained between these two sets of data was 0·025. Fig. 3 is a normal probability plot (Abrahams & Keve, 1971) representing the distribution of differences between data sets collected by the two techniques. The slope of the line is close to the ideal value of one, indicating that discrepancies between the two sets of data follow a normal distribution with standard deviations as calculated. This result is important because it means we can use the calculated standard deviations to demonstrate differences in signal-to-noise ratios. In the above test most intensities are greater than $2\sigma$ so no comparison of the sensitivities of the methods can be made.

The comparison of the two methods based on the dipeptide data has the advantage of checking on a relatively stable crystal with negligible absorption. Only data to 2 Å resolution were used since this corresponds to a limit common for protein crystals. Because data were collected with filtered Mo $K\alpha$ radiation, a modification of the method of background measurement was required. Initially, the backgrounds were evaluated from a $\theta$-dependent tabulation of backgrounds determined at the limits of the scan ranges of the weak reflections, but it was found that an improved fit of the background including the strong reflections was obtained by adding 0·036 times the count at the peak maximum to the original background. In addition, the standard deviation of the background was modified to $[\sigma_c^2 + (0{\cdot}017y_{max})^2]^{1/2}$. The data for the empirical peak width parameter $C_2'$ are given in Table 1 and details of the full-scan data collection are given by Stenkamp & Jensen (1974). The $D_I$ index between the data collected by the full-scan and step-scan techniques was 0·027, and a normal probability plot indicated that the calculated estimates of $\sigma(I)$ were reasonable.

In the test with the dipeptide data, it was feasible to check the use of an isotropic *vs* an anisotropic width parameter because the latter had a relatively large range. The test involved calculating for the step-scan data with both isotropic and anisotropic width parameters against the full-scan data omitting 14 reflections from the comparison because their backgrounds were badly affected by white radiation streaks. The effect of omitting these reflections was to reduce the value of anisotropic $D_I$ from 0·027 to 0·021; with an isotropic width parameter, $D_I$ increased to 0·025. This indicates that a substantial improvement was achieved with the anisotropic width parameter for limited-range, step-scan data.

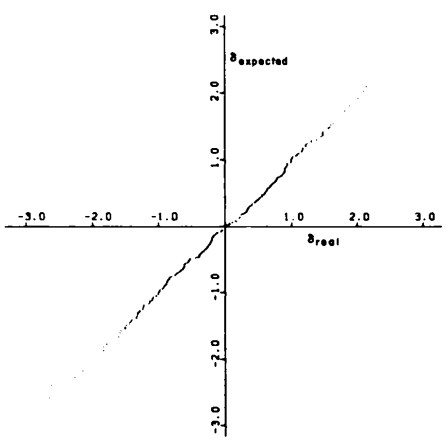


Fig. 3. Full normal probability plot for integrated intensities obtained by the full-scan method, $I_f$, and the limited-range, step-scan method, $I_l$, from a crystal of cytochrome cc'3 in a very low resolution shell. $\delta_{real} = (I_f - I_l)/(\sigma_f^2 - \sigma_l^2)$.

The data for the tests thus far were collected on a Picker, four-circle diffractometer operating under a modified FACS I data collecting system (Lenhert, 1975) with either Ni-filtered Cu $K\alpha$ or Nb-filtered Mo $K\alpha$ radiation. An additional test of the method was made with data collected on a Syntex $P2_1$, four-circle diffractometer with a graphite monochromator. In order to eliminate the influence of crystal deterioration and instrumental effects in this test, we extracted the limited-range, step-scan data from the profile data of the full scans.

Data for carboxyhemoglobin from *Glycera dibranchiata* ($a$ = 42·7, $b$ = 83·0, $c$ = 38·6 Å, $P2_12_12_1$) were collected within a spherical shell, $45{\cdot}0° < 2\theta < 45{\cdot}5°$, *i.e.* $d \simeq 2$ Å. The full scans were 2° in $2\theta$ at 0·5°/min. Backgrounds were measured at each end of the scan range for 2 min. A total of 386 reflections was measured of which 254 had intensities greater than $2\sigma$. The $D_I$ index for the symmetry-related reflections was 0·16.

The limited-range, step-scan data extracted from the full scans were equivalent to six 0·1° steps with a count time of 12 s for each step. The backgrounds for the step-scan data were obtained by fitting the backgrounds for the full-scan data by a tensor similar in form to the width parameter tensor.

The results of the width parameter determination are listed in Table 1 where it can be seen that the precision of the terms in the tensor for this test is much lower than that for the other structures. The number of reflections with $I > 2\sigma(I)$, however, was increased from 254 for the full-scan data to 324 for the limited-range, step-scan data, and $D_I$ for the symmetry-related reflections was 0·16, indicating agreement as good as that for the full-scan data. Fig. 4 is a normal probability plot showing that the differences between limited- and full-scan data, except for a few of the most negative ones, are random and consistent with the estimated standard deviations.

The times per reflection for the limited-range, step scan and for the full scan are 312 s and 480 s, respectively, for the *Glycera* hemoglobin data *including background counts*. Although requiring less than $\frac{2}{3}$ the time per reflection, the limited-range, step-scan data set had a substantially higher signal-to-noise ratio, and the number of reflections with $I > 2\sigma(I)$ increased by 28%.

## Discussion

Our experience with the limited-range, step-scan method suggests that reliable intensity data can be collected at a rate approximately twice that for the full-scan method, but certain precautions should be observed. In particular, if backgrounds are not measured for each reflection, care must be exercised in checking whether the background can be assumed to be a function only of $\theta$ or whether it should be fit by a function similar to that used for the width parameter or by some other function (Krieger, Chambers, Christoph, Stroud & Trus, 1974; Krieger & Stroud, 1976).

$A_{ij}$, $k$, and the standard deviation for an observation of unit weight, $S$, along with other information are listed in Table 1 for data sets of the structures cited above and for azurin. The eigenvalues of the width parameter tensors are tabulated in order to show the range of $C_2'$ covered. For comparative purposes, an isotropic width parameter and $S_{\rm iso}$ are listed for two of the four data sets. In the case of cytochrome cc'3, $S$ for the variable width function differs little from the value for the isotropic function and little is gained by using a variable width function. Note that the crystal dimensions for cytochrome cc'3 are uniform so that the crystal profile in the beam would not vary appreciably as the crystal orientation changed.

In the case of the dipeptide, the fit for the variable width function is substantially improved over the value for the isotropic function, but it still differs considerably from the ideal value of unity. Nevertheless, the agreement between the step-scan data and full-scan data is satisfactory as indicated by the agreement in $D_I$ values noted above.

For the *Glycera* hemoglobin and azurin data sets, the $S$ values are near unity, indicating a satisfactory fit of the tensor function within the limits imposed by the precision of the data.

In the tests reported here we have not allowed for changes in peak widths with time caused by changes in mosaic structure of the crystal resulting from crystal deterioration. This effect could be included by incorporating a factor to allow for variation in peak width as a function of crystal exposure to the X-ray beam.

The Gaussian profile assumed for the peaks is only an approximation of the actual peak shape, and it may be rather crude. Nevertheless, to the extent that the actual shapes of the X-ray peaks are uniform throughout a data set, the area under the Gaussian should be a good estimate of the integrated intensity on a relative scale. In fact, comparisons of the step-scan results with those from the full-scan for the cytochrome cc'3 and the dipeptide data sets suggest that errors resulting from the approximation are small. At high resolution where the $\alpha_1$–$\alpha_2$ separation becomes appreciable, fitting by a single Gaussian profile would be inadequate, but the method can readily be extended by using a pair of Gaussian profiles separated by the calculated amount.

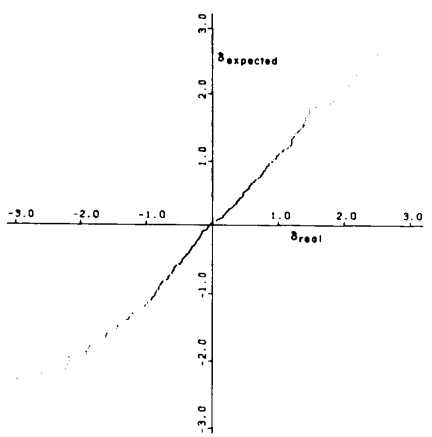


Fig. 4. Full normal probability plot as in Fig. 3 for *Glycera* hemoglobin data in a shell near 2 Å resolution.

This work was supported under USPHS Grants GM-10828, GM-13336 and AM-02528 from the National Institutes of Health. William M. Ringle provided technical assistance for the test of the method at the Johns Hopkins University.

## References

ABRAHAMS, S. C. & KEVE, E. T. (1971). *Acta Cryst.* A**27**, 157–165.

BLESSING, R. H., COPPENS, P. & BECKER, P. (1974). *J. Appl. Cryst.* **7**, 488–492.

BRUSCHI, M., LEGALL, J., HATCHIKIAN, E. C. & DUBOURDIEU, M. (1969). *Bull. Soc. Fr. Physiol. Veg.* **15**, 381–390.

DIAMOND, R. (1969). *Acta Cryst.* A**25**, 43–55.

HANSON, J. C., WATENPAUGH, K. D., SIEKER, L. C. & JENSEN, L. H. (1973). *Abstr. Am. Crystallogr. Assoc.* p. 55.

KRIEGER, M., CHAMBERS, J. L., CHRISTOPH, G. G., STROUD, R. M. & TRUS, B. L. (1974). *Acta Cryst.* A**30**, 740–748.

KRIEGER, M. & STROUD, R. M. (1976). *Acta Cryst.* A**32**, 653–656.

LEHMANN, M. S. & LARSEN, F. K. (1974). *Acta Cryst.* A**30**, 580–584.

LENHERT, P. G. (1975). *J. Appl. Cryst.* **8**, 568–570.

SIEKER, L. C. & JENSEN, L. H. (1971). *Abstr. Am. Crystallogr. Assoc.* p. 69.

STENKAMP, R. E. & JENSEN, L. H. (1974). *Acta Cryst.* B**30**, 1541–1545.

TICKLE, I. J. (1975). *Acta Cryst.* B**31**, 329–331.

WATENPAUGH, K. D., SIEKER, L. C. & JENSEN, L. H. (1973). *Proc. Natl Acad. Sci. USA*, **70**, 3857–3860.

WATENPAUGH, K. D., SIEKER, L. C., JENSEN, L. H., LEGALL, J. & DUBOURDIEU, M. (1972). *Proc. Natl Acad. Sci. USA*, **69**, 3185–3188.

WYCKOFF, H. W., DOSCHER, M., TSERNOGLOU, D., INAGAMI, T., JOHNSON, L. N., HARDMAN, K. D., ALLWELL, N. M., KELLY, D. M. & RICHARDS, F. M. (1967). *J. Mol. Biol.* **27**, 563–578.